

# Accepted Manuscript

Evaluating the feasibility of using Sentinel-2 imagery for water clarity assessment in a reservoir

Matias Bonansea, Micaela Ledesma, Raquel Bazán, Anabella Ferral, Alba German, Patricia O'Mill, Claudia Rodriguez, Lucio Pinotti



PII: S0895-9811(19)30222-6

DOI: <https://doi.org/10.1016/j.jsames.2019.102265>

Article Number: 102265

Reference: SAMES 102265

To appear in: *Journal of South American Earth Sciences*

Received Date: 9 May 2019

Revised Date: 4 July 2019

Accepted Date: 5 July 2019

Please cite this article as: Bonansea, M., Ledesma, M., Bazán, R., Ferral, A., German, A., O'Mill, P., Rodriguez, C., Pinotti, L., Evaluating the feasibility of using Sentinel-2 imagery for water clarity assessment in a reservoir, *Journal of South American Earth Sciences* (2019), doi: <https://doi.org/10.1016/j.jsames.2019.102265>.

This is a PDF file of an unedited manuscript that has been accepted for publication. As a service to our customers we are providing this early version of the manuscript. The manuscript will undergo copyediting, typesetting, and review of the resulting proof before it is published in its final form. Please note that during the production process errors may be discovered which could affect the content, and all legal disclaimers that apply to the journal pertain.

# 1 **Evaluating the feasibility of using Sentinel-2 imagery for water clarity** 2 **assessment in a reservoir**

3 Matias Bonansea <sup>a,b\*</sup>, Micaela Ledesma <sup>b</sup>, Raquel Bazán <sup>c</sup>, Anabella Ferral <sup>d</sup>, Alba German  
4 <sup>d,e</sup>, Patricia O'Mill <sup>c,e</sup>, Claudia Rodriguez <sup>b</sup>, Lucio Pinotti <sup>a,f</sup>

5  
6 <sup>a</sup> Instituto de Ciencias de la Tierra, Biodiversidad y Sustentabilidad Ambiental (ICBIA),  
7 Consejo Nacional de Investigaciones Científicas y Técnicas (CONICET), Argentina.

8 <sup>b</sup> Departamento de Estudios Básico y Agropecuarios, Facultad de Agronomía y Veterinaria  
9 (FAyV), Universidad Nacional de Río Cuarto (UNRC).

10 <sup>c</sup> Departamento de Ingeniería Química y Aplicada, Facultad de Ciencias Exactas Físicas y  
11 Químicas, Universidad Nacional de Córdoba (UNC).

12 <sup>d</sup> Instituto de Altos Estudios Espaciales Mario Gulich, Centro Espacial Teófilo Tabanera,  
13 Comisión Nacional de Actividades Espaciales (CONAE).

14 <sup>e</sup> Administración de Recursos de Recursos Hídricos (APRHI), Ministerio de Servicios  
15 Públicos, Provincia de Córdoba.

16 <sup>f</sup> Departamento de Geología, Facultad de Ciencias Exactas, Físico-Químicas y Naturales,  
17 UNRC.

18 (\* Corresponding author). Ruta Nacional N° 36 Km 601. (5800) Río Cuarto, Córdoba,  
19 Argentina. E-mail: mbonansea@ayv.unrc.edu.ar. Tel: +54 358 46 76512.

## 20 **Abstract**

21  
22 The new Sentinel-2 satellites present a significant scientific opportunity for the study of  
23 water quality. The objective of this study was to evaluate the suitability of Sentinel-2  
24 imagery for estimating and mapping Secchi disk transparency (SDT) in Río Tercero  
25 reservoir (Córdoba-Argentina). Field observations and a dataset of atmospherically  
26 corrected Sentinel-2 images were used to generate and validate an algorithm to estimate  
27 water clarity in the studied reservoir. As a real application of the used methodology, the  
28 validated algorithm was used to obtain a spatial representation of water clarity in the  
29 reservoir during sampling campaigns. Results demonstrate capabilities of Sentinel-2  
30 mission to make a substantial contribution to the current assessment and understanding of  
31 aquatic systems by estimating and mapping a water quality characteristic.

32 **Keywords:** Aquatic system; Remote sensing; Statistical algorithm; Sentinel-2  
33 mission; Water quality.

34

## 35 **1. Introduction**

36 Lakes and reservoirs have important functions in the environment. Like many  
37 other ecosystems, these environments are threatened by the synergistic effects of multiple  
38 co-occurring environmental pressures, including human activities, nutrient enrichment,  
39 inorganic and organic pollution, and climate change (Palmer et al., 2015; Dörnhöfer and  
40 Oppelt, 2016; Ferral et al., 2017; El-Serehy et al., 2018). Therefore, it is imperative to  
41 develop new water quality monitoring tools for an efficient management of water resources  
42 (Wang et al., 2017).

43 Satellite remote sensing can improve water quality monitoring and increase the  
44 rapid detection of environmental threats, such as eutrophication or harmful algal blooms,  
45 due to its time- and cost-effectiveness over large areas as well as remote locations. This is  
46 of special interest in the Caribbean and South America region, where there are difficulties  
47 in obtaining basic information on water quality (Matthews, 2011; Gonzalez-Marquez et al.,  
48 2018). Furthermore, during the last few years, there is an increasing international interest  
49 on the new generation of medium resolution (10–30 m) Earth observation satellites to open  
50 a complete new era in the remote sensing of inland waters (Concha and Schott, 2016;  
51 Dörnhöfer and Oppelt, 2016; Sovdat et al., 2019). Among these new satellites, the  
52 Sentinel-2 mission, developed by the European Space Agency's (ESA) Copernicus  
53 program, provides improved continuity for Landsat and SPOT observations and improves  
54 data availability for users since it can be used to support global land services including  
55 monitoring vegetation, soil and aquatic systems (Drusch et al., 2012; Du et al., 2016; Wang  
56 and Atkinson, 2018).

57 The Sentinel-2 mission carries a push-broom MultiSpectral Instrument (MSI)

58 aboard Sentinel-2A and Sentinel-2B twin satellites which were launched on 23 June 2015  
59 and 7 March 2017, respectively (Sola et al., 2018). The Sentinel-2 mission presents high  
60 spatial resolution, multiple spectral bands, short revisit times, and an open data policy,  
61 which has made it a rich satellite data archive available to the general public (Sovdat et al.,  
62 2019). The pair of Sentinel-2 satellites presents a significant scientific opportunity for the  
63 study of aquatic ecosystems by monitoring and mapping water quality constituents in near  
64 shore coastal and inland waters. However, Sentinel-2 derived-products require further  
65 community-wide validations to ensure performance under different environmental  
66 conditions.

67 The objective of this study was to evaluate the suitability of Sentinel-2 imagery for  
68 estimating and mapping Secchi disk transparency (SDT) in Río Tercero reservoir  
69 (Córdoba-Argentina). We focused on SDT, a common measurement of water clarity, since  
70 it is a widely used metric of lakes and reservoirs water quality closely associated with  
71 water quality indicators such as trophic status, chlorophyll-a, lake productivity and total  
72 phosphorus (Carlson, 1977; Olmanson et al., 2016; Shang et al., 2016). Further, due to its  
73 simplicity and low-cost facilities, SDT is commonly used by many volunteer monitoring  
74 programs and it is one of the most widely water quality characteristic estimated by remote  
75 sensing (Kloiber et al., 2002; Olmanson et al., 2008).

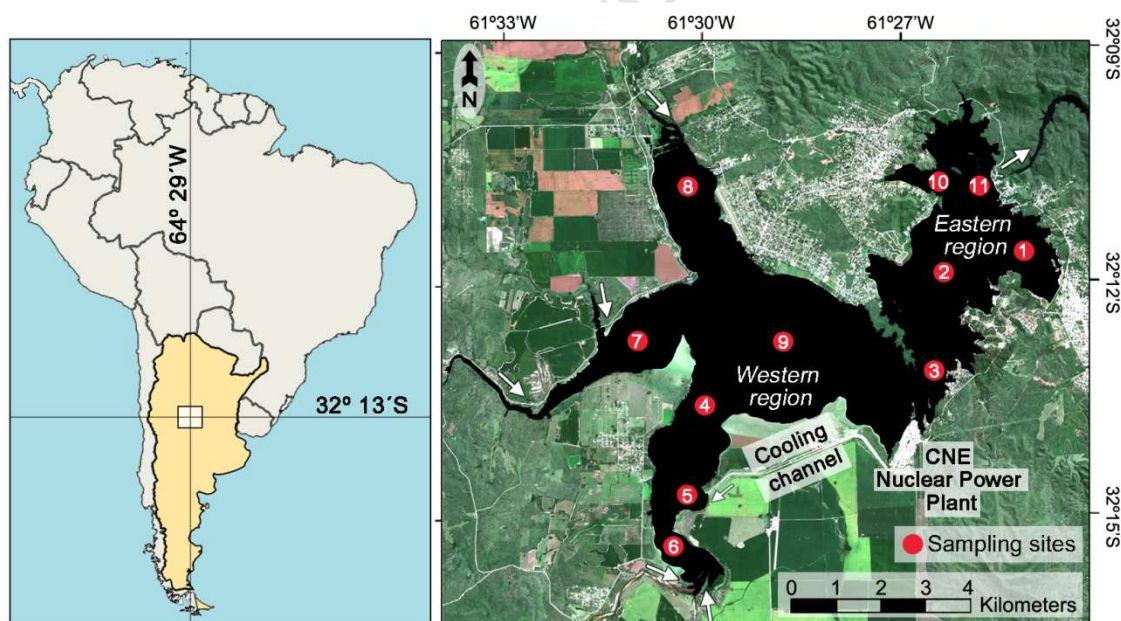
76

## 77 **2. Methodology**

### 78 **2.1. Study area**

79 The Río Tercero reservoir is located in the province of Córdoba (Argentina) (Figure  
80 1). This reservoir has an area of 46 km<sup>2</sup>, a volume of 10 hm<sup>3</sup>, a maximum and mean depth  
81 of 46.5 and 12.2 m respectively (Mariazzi et al., 1992). The Río Tercero reservoir is  
82 divided in two regions by a strait. The western region has three branches where rivers flow,

83 while the eastern region presents the only effluent called Tercero river. The Río Tercero  
 84 reservoir is one of the most important artificial reservoirs in the central region of Argentina  
 85 since it plays an important ecological and socio-economical role in the development of  
 86 cities and towns located nearby. In this sense, the studied reservoir has multiple purposes,  
 87 such as water supply for approximately 20000 inhabitants, power generation, flood control,  
 88 irrigation, tourism and recreational activities (Mariazzi et al., 1992). However, in the last  
 89 two decades, water quality of the reservoir is declining, reducing its multi-purpose value  
 90 (Bonansea et al., 2016). In 1986 a nuclear power plant (CNE: 600 MWa) was installed.  
 91 Water for cooling the nuclear reactor is taken from the middle section of the reservoir and  
 92 is returned to the western basin by a 5 km long open-sky channel (Bonansea et al., 2015b).  
 93 In 2015, the power plant was stopped since it is in a reconditioning process to extend its  
 94 useful life.



95  
 96 **Fig. 1.** Study area and location of sampling sites.

## 97 **2.2. Field campaigns**

98 Sampling campaigns were conducted on February 28, 2018; March 14, 2018;  
 99 August 28, 2018; October 17, 2018; February 14, 2019; and March 24, 2019 at eleven  
 100 sampling sites (Figure 1). Coordinates of sample sites were recorded using a GPS device.

101 Water clarity was measured using a standard 20 cm diameter Secchi disk from the shady  
 102 side of a boat to avoid any undesirable effects of water surface reflection. One-way  
 103 analysis of variance (ANOVA) was performed as a first approach to compare the  
 104 significant spatial and temporal variation of SDT values measured in the reservoir ( $p <$   
 105  $0.05$ ; least significance difference, LSD).

106

### 107 **2.3. Remote sensing data and processing**

108 In the present study, the used remote sensing data was acquired by Sentinel-2A and  
 109 B satellites. As we have previously mentioned, the Sentinel-2 satellites carry the MSI  
 110 sensor which measures the reflected solar spectral radiance in thirteen spectral bands  
 111 ranging from the visible (VIS) to the shortwave infrared (SWIR) bands at 3 different  
 112 spatial resolutions (Table 1). The radiometric resolution of MSI sensor is 12-bit and it  
 113 incorporates three new red edge spectral bands (RE1, RE2, RE3) which would improve the  
 114 accuracy of estimating various biophysical variables (Drusch et al., 2012; Traganos and  
 115 Reinartz, 2018).

116

117

**Table 1.** Band specifications for Sentinel-2 MSI sensor.

Band	Spatial resolution (m)	Wavelength (nm)
1- Aerosol	60	433-453
2- Blue	10	458-523
3- Green	10	543-578
4- Red	10	650-680
5- Red edge (RE) 1	20	698-713
6- RE2	20	733-748
7- RE3	20	773-793
8- Near infrared (NIR)	10	785-900

8a- Near infrared narrow (NIRn)	20	855-875
9- Water vapour	60	935-955
10- Shortwave infrared (SWIR)/Cirrus	60	1360-1390
11- SWIR-1	20	1565-1655
12- SWIR-2	20	2100-2280

118

119 Synchronous to fieldwork activities, cloud-free Sentinel-2A/B images of the study  
120 area were downloaded from the USGS Global Visualization Viewer  
121 (<http://glovis.usgs.gov>). Six images acquired on March 1, 2018; March 14, 2018; August  
122 28, 2018; October 16, 2018; February 14, 2019; and March 24, 2019 were downloaded as  
123 Level-1C products. Level-1C data corresponds to Top-Of-Atmosphere (TOA) reflectance  
124 values after the application of radiometric and geometric corrections (including  
125 orthorectification and spatial registration) (Sola et al., 2018).

126 Atmospheric correction of satellite data was conducted in order to develop a  
127 sufficiently reliable relationship between water quality variables and remote sensing data  
128 (Rozo et al., 2014; Bonansea et al., 2015). Atmospheric correction of Sentinel-2 imagery  
129 was performed using Sen2Cor module (version 2.5.5) within the Sentinel-2 Toolbox  
130 integrated in the Sentinel Application Platform software (SNAP), which is developed and  
131 freely distributed by ESA (ESA, 2018). Using Sen2Cor model each TOA Level-1C  
132 Sentinel-2 image was transformed into a Bottom-of-Atmosphere (BOA) Level-2A product  
133 (Steinhausen et al., 2018). Further details on Sen2Cor processor and its calibration can be  
134 obtained in Müller-Wilm (2017) and Richter et al. (2017). After atmospheric correction,  
135 RE1/2/3 bands and SWIR-1/2 bands were resampled to match the 10 m resolution of the  
136 other bands. Once preprocessing was complete, the normalized difference water index  
137 (NDWI) was used to mask out terrestrial features creating water-only images (McFeeters,  
138 1996). The NDWI algorithm was used to delineate the reservoir surface on each image,  
139 while background information was restricted.

140

141 **2.4. Model development**

142           Once image processing was complete, atmospheric corrected values from MSI  
143 bands were used to develop relationships with measured SDT data using linear regression  
144 analysis, which is defined as a statistical technique used to relate a set of independent  
145 variables (BOA values of MSI bands) and a response variable (SDT measured in Río  
146 Tercero reservoir) by fitting a linear equation to the observed data (Jobson, 2012). The  
147 dataset used in this study was divided into two groups, a calibration subset (sampling  
148 campaigns performed on February 28, 2018; March 14, 2018; August 28, 2018; October  
149 17, 2018) and a validation subset (sampling campaign performed on February 14, 2019;  
150 and March 24, 2019). The mean BOA reflectance value from a 3 x 3 grid centred on the  
151 GPS coordinates of the *in-situ* measurement sites was used to correlate with ground data.  
152 Based on previous studies, single band and band ratios were tested to ensure robust  
153 algorithms (Matthews, 2011). Using the calibration subset, algorithms to estimate SDT  
154 were generated using forward step-wise multiple regression analysis ( $p < 0.05$ ). Standard  
155 regression assumptions were verified graphically and statistically. The Shapiro Wilks's test  
156 ( $p > 0.05$ ) was used to prove assumption of normality. Levene's test ( $p > 0.05$ ) was used to  
157 verify homogeneity of variances.

158           According to Mathews (2011) and Politi et al. (2015) researchers developed many  
159 different retrieval algorithms to estimate SDT, due to the fact that the best model varies  
160 from one reservoir to another according to water conditions. Thus, we chose not to employ  
161 preconceived models to estimate SDT and a wide variety of candidate algorithms were  
162 tested. Additionally, different goodness-of-fit measures, including the adjusted R-squared  
163 value ( $R^2$ ), the bias (mean difference between estimated and observed SDT), and the root  
164 mean square error (RMSE) were calculated to obtain an estimate of the error associated  
165 with the estimations. The model with the greatest  $R^2$  and the lowest Bias and RMSE was



166 selected to retrieve SDT in the entire reservoir surface. The predictive capability of the  
 167 model was also assessed by comparing the predicted and the observed SDT values of the  
 168 validation subset by simple regression analysis. Finally, to assess water clarity in the  
 169 reservoir, quantitative maps were created applying the selected model to the used imagery.

170

### 171 3. Results and discussion

#### 172 3.1. Field data

173 The basic statistics of SDT measured in R o Tercero reservoir during the sampling  
 174 campaigns are summarized in Table 2.

175

176 **Table 2.** Sampling dates and basic statistics of water clarity measured in R o Tercero reservoir.

Sampling campaign	Acquisition image date	Difference in days	SDT values	
			Mean±Sd.	Range
February 28, 2018	March 1, 2018	1	2.00 ±0.74	0.50-3.00
March 14, 2018	Mach 14, 2018	0	1.83±0.64	0.75-2.50
August 28, 2018	August 28, 2018	0	1.93±0.86	0.60-3.25
October 16, 2018	October 17, 2018	1	1.83±0.81	0.50-2.90
February 14, 2019	February 14, 2019	0	1.60±0.74	0.60-2.50
March 24, 2019	March 24, 2019	0	2.12±0.81	0.75-3.25

177 Sd.: Standard deviation.

178

179 ANOVA did not showed significant differences between sampling campaigns ( $p =$   
 180  $0.71$ ). However, this technique indicated significant differences when sampling sites were  
 181 compared ( $p > 0.01$ ). Sampling sites located in the western region of the reservoir (Sites 4  
 182 to 9) were significantly lower than those located in the eastern region (Sites 1, 2, 3, 10, and  
 183 11).

184

#### 185 3.2. Algorithms

186 Regression model was performed using the calibration subset which contained 44

187 pairs of field and satellite data. Thus, measured SDT values were used to find the best  
 188 combination of MSI spectral band or band ratios to estimate water clarity in Río Tercero  
 189 reservoir. Eq. (1) shows the best model developed to predict SDT in the reservoir which  
 190 included a combination of red edge and near infrared bands of MSI sensor ( $R^2=0.86$ ):

$$191 \quad SDT = 1.79 - 134.15 * Band_{RE1} + 157.72 * Band_{NIR} + 0.53 * \frac{Band_{RE3}}{Band_{NIRn}} \quad Eq. (1)$$

192 where  $Band_{RE1}$ ,  $Band_{NIR}$ ,  $Band_{RE3}$ , and  $Band_{NIRn}$  are the atmospherically corrected BOA  
 193 values of MSI spectral bands.

194

195 Figure 2 shows the comparison between field data and SDT values estimated by  
 196 Sentinel-2 satellite. Figure 2a, which represents comparison between observed and  
 197 estimated SDT values used for model development, shows a good fit obtained from  
 198 regression analysis ( $R^2 = 0.85$ , Bias = 0.03 m, and RMSE = 0.28 m) and a good agreement  
 199 between the gradient and intercept of the regression line. The capacity of the generated  
 200 algorithm was also validated comparing values of SDT measured in the field and SDT  
 201 values predicted by applying the algorithm on BOA values of Sentinel-2 images of the  
 202 validation dataset (Figure 2b). In this case, the used goodness-of-fit measures also confirms  
 203 the robustness and the high predictive capacity of the developed algorithm and produce an  
 204 acceptable error associated with the estimations ( $R^2 = 0.81$ , Bias = 0.12 m, and RMSE =  
 205 0.38 m).

206

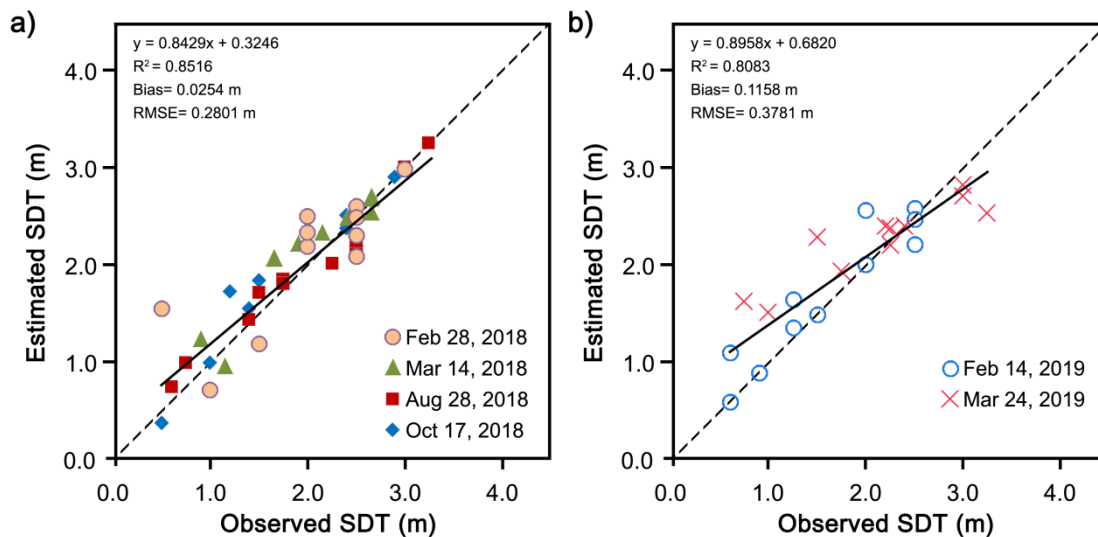
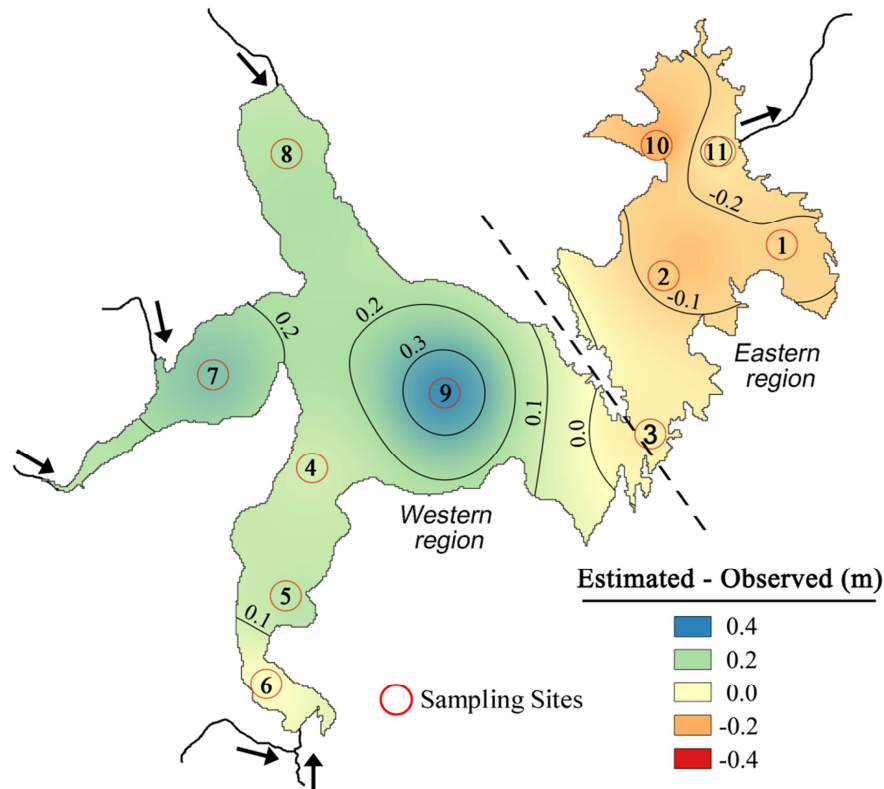


**Fig. 2.** Plots of observed versus estimated SDT values in Río Tercero reservoir with 1:1 fit line generated with a) calibration dataset and b) validation dataset.

Figure 3 shows the spatial distribution of simulation mean errors during sampling campaigns. Comparing the mean difference between estimated and observed values of SDT, it was observed that the developed algorithm tended to generate a slight overestimation of SDT values when observed SDT values were low. On the other hand, when observed SDT values were high, the selected algorithm generated an underestimation of SDT values. This is evident in Figure 3, which shows that in the western region of the reservoir, where lower values of water transparency were found, the overestimation of SDT values was evident by a positive difference between estimated versus observed SDT values. In the eastern region of the reservoir, the negative values of simulated errors demonstrated the underestimation generated by the used algorithm. Figure also shows that the central region of the reservoir presented the lower difference between estimated and observed water transparency values.



223

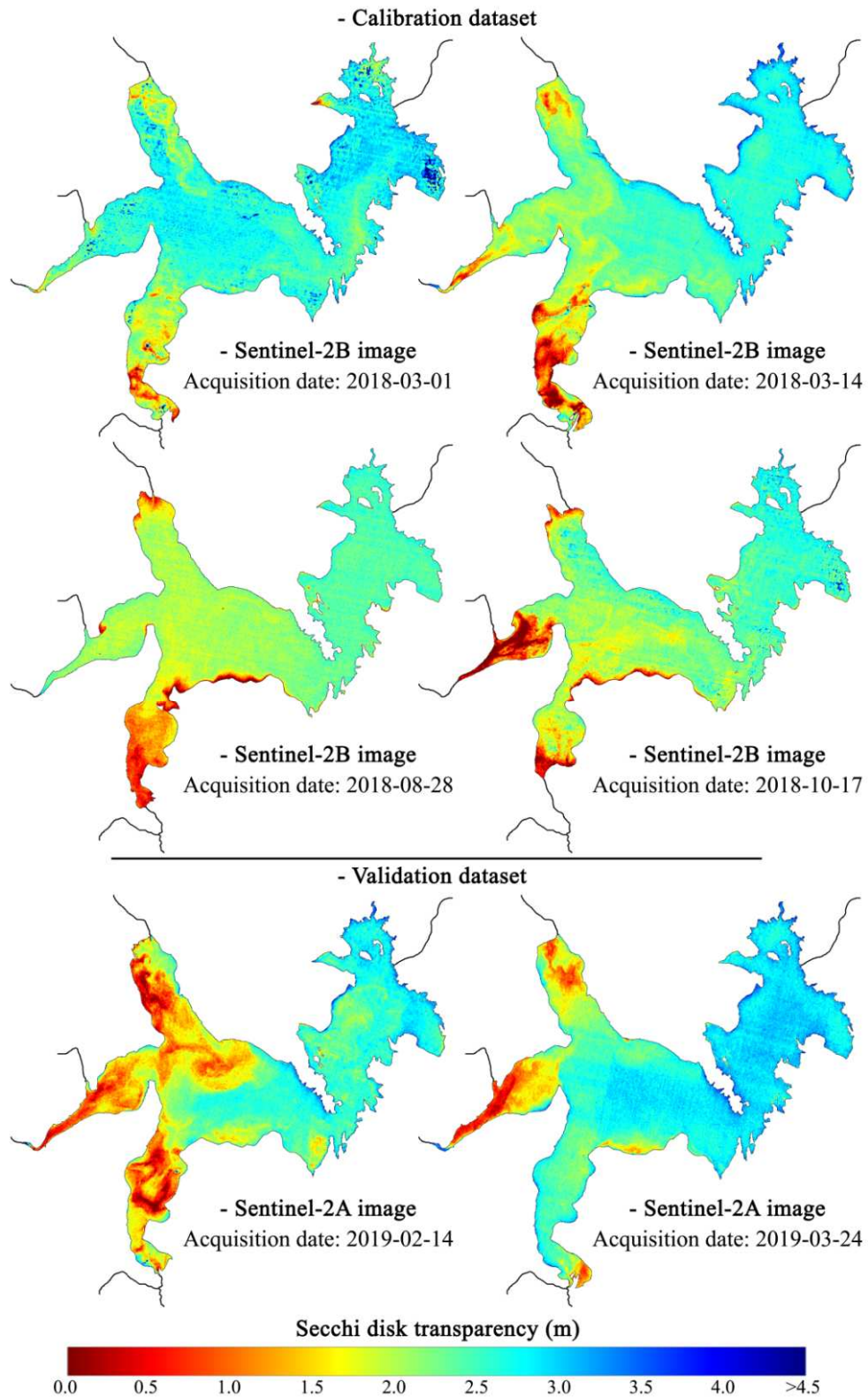
224 **Fig. 3.** Spatial distribution of mean difference between estimated versus observed SDT values in  
 225 Río Tercero reservoir during sampling campaigns.

226

### 227 3.3. Algorithm implementation

228 As a real application of remote sensing techniques, the validated algorithm was  
 229 applied to the used Sentinel-2 imagery obtaining a spatial representation of water clarity in  
 230 Río Tercero reservoir during sampling campaigns (Figure 4). This Figure shows that high-  
 231 quality products can be derived from Sentinel-2 imagery. Coinciding with field data,  
 232 satellite imagery shows a spatial pattern of water clarity with lower values of SDT in the  
 233 western region and increasing towards the eastern region of the reservoir. This longitudinal  
 234 pattern could be associated with river runoff which delivers higher loads of suspended  
 235 materials and dissolved solids into the western region of the reservoir that decrease the  
 236 penetration of light and contribute to the reduction of water clarity. This situation is more  
 237 evident close to river inputs. The opposite situation occurs in the eastern region of the  
 238 reservoir where deeper waters and rapid sedimentation allow the measure of higher values

239 of SDT. A similar spatial pattern of lower water clarity near river inflows and increasing  
240 with distance was found by Bonansea et al. (2015) in this reservoir and by Bazán et al.  
241 (2005), Giardino et al. (2010) and Guan et al. (2011) in different water bodies. Finally, as  
242 results show the generated algorithm could be used in the both Sentinel-2 satellites, thus  
243 the revisit time over the studied area could be reduced to 5 days, which is a benefit for  
244 operational uses and decision-making activities (Pahlevan et al., 2017, Sovdat et al., 2019).  
245



246

247

**Fig. 4.** Graphic representation of SDT in Río Tercero reservoir by applying Eq. (1) on atmospherically corrected values extracted from Sentinel-2 images.

248

249

250

Different multi-resolution satellites have been successfully used to estimate water

251 clarity and other water quality variables of inland waters (Matthews, 2011; Villar et al.,  
252 2013; Dörnhöfer and Oppelt, 2016). However, as we have previously mentioned, there is  
253 an increasing international interest for the evaluation of the potential of new satellite  
254 systems and its derived products. In the present study, field data and Sentinel-2 imagery  
255 were used to generate a relevant and validated empirical algorithm for estimating and  
256 mapping water clarity in one of the most important reservoir of the central region of  
257 Argentina. Although we can confirm that the methodology used in the present study is  
258 adequate to estimate water clarity, it should be noted that the accuracy of the development  
259 algorithm is limited. Thus, for further validation, more simultaneous field observations  
260 with overpass time of Sentinel-2 must be compared for improving the accuracy and  
261 precision of the coefficients of the generated algorithm. Further, due to the influence of the  
262 nuclear power plant on water quality (Bonansea et al. 2015; 2018), we recommend that it  
263 must be taken into account when it is operative again for water quality assessment.

264

#### 265 **4. Conclusions**

266 This study demonstrates capabilities of Sentinel-2 mission to make a substantial  
267 contribution to the current assessment and understanding of aquatic systems by estimating  
268 and mapping a water quality characteristic in a reservoir of Argentina.

269 An algorithm to estimate SDT, a common measurement of water clarity, was  
270 generated and validated with high goodness-of-fit measures that confirms its robustness  
271 and its high predictive capacity ( $R^2 = 0.81$ , bias = 0.12 m, and RMSE = 0.38 m). Results  
272 also show that the produced water clarity maps enable for the interpretation of the  
273 behaviour of the variable in the whole reservoir. However, further research study with a  
274 larger data set is needed for a multi-temporal evaluation.

275

276 **Acknowledgements**

277 This study was supported by the CONICET and the Agencia Nacional de  
278 Promoción Científica y Tecnológica [grant number PICT-1408, 2015]; and SECyT-UNRC  
279 (Secretaría de Ciencia y Técnica, Universidad Nacional de Río Cuarto) [grant number Res.  
280 18A369, 2016]. The authors would like to thank Nautical Security Direction of Córdoba  
281 province for their collaboration in sampling campaigns.

282

283 **References**

- 284 Bazán, R., Corral, M., Pagot, M., Rodríguez, A., Oroná, C., Rodríguez, M., Larrosa, N.,  
285 Cossavella, A., del Olmo, S., Bonfanti, E., Busso, F., 2005. Teledetección y modelado  
286 numérico para el análisis de la calidad de agua del embalse Los Molinos. Ingeniería  
287 hidráulica en México, 20(2), 121–135.
- 288 Bonansea, M., Rodriguez, M., Pinotti, L., Ferrero, S., 2015. Using multi-temporal Landsat  
289 imagery and linear mixed models for assessing water quality parameters in Río  
290 Tercero reservoir (Argentina). Remote Sensing of Environment, 158, 28–41.
- 291 Bonansea, M., Ledesma, C., Rodriguez, M., 2016. Assessing the impact of land use and  
292 land cover on water quality in the watershed of a reservoir. Applied Ecology and  
293 Environmental Research, 14(2), 447–456.
- 294 Bonansea, M., Bazán, R., Ferrero, S., Rodríguez, C., Ledesma, C., Pinotti, L., 2018.  
295 Multivariate statistical analysis for estimating surface water quality in reservoirs.  
296 International Journal of Hydrology Science and Technology, 8(1), 52–68.
- 297 Carlson, R., 1977. A trophic state index for lakes. Limnology and oceanography, 22(2),  
298 361–369.
- 299 Concha, J., Schott, J., 2016. Retrieval of color producing agents in Case 2 waters using  
300 Landsat 8. Remote Sensing of Environment, 185, 95–107.



- 301 Dörnhöfer, K., Oppelt, N., 2016. Remote sensing for lake research and monitoring—Recent  
302 advances. *Ecological Indicators*, 64, 105–122.
- 303 Drusch, M., Del Bello, U., Carlier, S., Colin, O., Fernandez, V., Gascon, F., Hoersch, B.,  
304 Isola, C., Laberinti, P., Martimort, P., A.Meygret, A., Spoto, F., Sy, O., Marchese, F.,  
305 Bargellini, P., 2012. Sentinel-2: ESA's optical high-resolution mission for GMES  
306 operational services. *Remote Sensing of Environment*, 120, 25–36.
- 307 Du, Y., Zhang, Y., Ling, F., Wang, Q., Li, W., Li, X., 2016. Water bodies' mapping from  
308 Sentinel-2 imagery with modified normalized difference water index at 10-m spatial  
309 resolution produced by sharpening the SWIR band. *Remote Sensing*, 8(4), 354.
- 310 ESA. 2018. SNAP – ESA Sentinel Application Platform v6.0. <http://step.esa.int/main/>.
- 311 Ferral, A., Solis, V., Frery, A., Orueta, A., Bernasconi, I., Bresciano, J., Scavuzzo, C. M.,  
312 2017. Spatio-temporal changes in water quality in an eutrophic lake with artificial  
313 aeration. *Journal of Water and Land Development*, 35(1), 27–40.
- 314 Giardino, C., Bresciani, M., Villa, P., Martinelli, A., 2010 Application of remote sensing in  
315 water resource management: the case study of Lake Trasimeno, Italy. *Water  
316 Resources Management*, 24(14), 3885–3899.
- 317 González-Márquez, L., Torres-Bejarano, F., Torregroza-Espinosa, A., Hansen-Rodríguez,  
318 I., Rodríguez-Gallegos, H., 2018. Use of LANDSAT 8 images for depth and water  
319 quality assessment of El Guájaro reservoir, Colombia. *Journal of South American  
320 Earth Sciences*, 82, 231–238.
- 321 Guan, X., Li, J., Booty, W., 2011. Monitoring lake Simcoe water clarity using Landsat-5  
322 TM images. *Water Resources Management*, 25(8), 2015–2033.
- 323 El-Serehy, H., Abdallah, H., Al-Misned, F., Al-Farraj, S., Al-Rasheid, K., 2018. Assessing  
324 water quality and classifying trophic status for scientifically based managing the water  
325 resources of the Lake Timsah, the lake with salinity stratification along the Suez  
326 Canal. *Saudi Journal of Biological Sciences*, 25(7), 1247–1256.

- 327 Jobson, J., 2012. Applied multivariate data analysis: volume II: Categorical and  
328 Multivariate Methods. Springer Science & Business Media.
- 329 Kloiber, S., Brezonik, P., Olmanson, L., Bauer, M., 2002. A procedure for regional lake  
330 water clarity assessment using Landsat multispectral data. *Remote Sensing of*  
331 *Environment*, 82 (1), 38–47.
- 332 Mariazzi, A., Donadelli, J., Arenas, P., Di Siervi, M., Bonetto, C., 1992. Impact of a  
333 nuclear power plant on water quality of Embalse del Río Tercero reservoir (Córdoba,  
334 Argentina). *Hidrobiologia*, 246, 129-140.
- 335 Matthews, M., 2011. A current review of empirical procedures of remote sensing in inland  
336 and near-coastal transitional waters. *International Journal of Remote Sensing*, 32(21),  
337 6855–6899.
- 338 McFeeters, S., 1996 The use of normalized difference water index (NDWI) in the  
339 delineation of open water features. *International Journal of Remote Sensing*, 17, 1425–  
340 1432.
- 341 Müller-Wilm, U., 2016. Sentinel-2 MSI – Level-2A Prototype Processor Installation and  
342 User Manual. Telespazio VEGA Deutschland GmbH, Darmstadt.
- 343 Olmanson L., Bauer, M., Brezonik, P., 2008. A 20-year Landsat water clarity census of  
344 Minnesota's 10,000 lakes. *Remote Sensing of Environment*, 112(11), 4086–4097.
- 345 Olmanson, L., Brezonik, P., Finlay, J. Bauer, M., 2016 Comparison of Landsat 8 and  
346 Landsat 7 for regional measurements of CDOM and water clarity in lakes. *Remote*  
347 *Sensing of Environment*, 185, 119–128.
- 348 Palmer, S., Kutser, T., Hunter, P., 2015. Remote sensing of inland waters: Challenges,  
349 progress and future directions. *Remote Sensing of Environment*, 157, 1–8.
- 350 Pahlevan, N., Sarkar, S., Franz, B., Balasubramanian, S., He, J., 2017. Sentinel-2  
351 MultiSpectral Instrument (MSI) data processing for aquatic science applications:  
352 Demonstrations and validations. *Remote Sensing of Environment*, 201, 47–56.

- 353 Politi, E., Cutler, M., Rowan, J., 2015. Evaluating the spatial transferability and temporal  
354 repeatability of remote-sensing-based lake water quality retrieval algorithms at the  
355 European scale: a meta-analysis approach. *International Journal of Remote Sensing*,  
356 36(11), 2995–3023.
- 357 Richter, R., Louis, J., Berthelot, B., 2017. Sentinel-2 MSI–Level 2A Products Algorithm  
358 Theoretical Basis Document.  
359 [https://earth.esa.int/c/document\\_library/get\\_file?folderId=349490&name=DLFE-](https://earth.esa.int/c/document_library/get_file?folderId=349490&name=DLFE-4518.pdf)  
360 [4518.pdf](https://earth.esa.int/c/document_library/get_file?folderId=349490&name=DLFE-4518.pdf).
- 361 Rozo, M., Nogueira, A., Castro, C., 2014. Remote sensing-based analysis of the planform  
362 changes in the Upper Amazon River over the period 1986–2006. *Journal of South*  
363 *American Earth Sciences*, 51, 28–44.
- 364 Shang, S., Lee, Z., Shi, L., Lin, G., Wei, G., Li, X., 2016. Changes in water clarity of the  
365 Bohai Sea: Observations from MODIS. *Remote Sensing of Environment*, 186, 22–31.
- 366 Sola, I., García-Martín, A., Sandonís-Pozo, L., Álvarez-Mozos, J., Pérez-Cabello, F.,  
367 González-Audícana, M., Llovería, R., 2018. Assessment of atmospheric correction  
368 methods for Sentinel-2 images in Mediterranean landscapes. *International Journal of*  
369 *Applied Earth Observation and Geoinformation*, 73, 63–76.
- 370 Sovdat, B., Kadunc, M., Batič, M., Milčinski, G., 2019. Natural color representation of  
371 Sentinel-2 data. *Remote Sensing of Environment*, 225, 392–402.
- 372 Steinhausen, M., Wagner, P., Narasimhan, B., Waske, B., 2018. Combining Sentinel-1 and  
373 Sentinel-2 data for improved land use and land cover mapping of monsoon regions.  
374 *International Journal of Applied Earth Observation and Geoinformation*, 73, 595–604.
- 375 Traganos, D., Reinartz, P., 2018. Mapping Mediterranean seagrasses with Sentinel-2  
376 imagery. *Marine Pollution Bulletin*, 134, 197–209.

- 377 Villar, R., Martinez, J., Le Texier, M., Guyot, J., Fraizy, P., Meneses, P., de Oliveira, E.,  
378 2013. A study of sediment transport in the Madeira River, Brazil, using MODIS  
379 remote-sensing images. *Journal of South American Earth Sciences*, 44, 45–54.
- 380 Wang, Q., Atkinson, P., 2018. Spatio-temporal fusion for daily Sentinel-2 images. *Remote*  
381 *Sensing of Environment*, 204, 31–42.
- 382 Wang, X., Zhang, F., Ghulam, A., Trumbo, A., Yang, J., Ren, Y., Jing, Y., 2017.  
383 Evaluation and estimation of surface water quality in an arid region based on EEM-  
384 PARAFAC and 3D fluorescence spectral index: A case study of the Ebinur Lake  
385 Watershed, China. *Catena*, 155, 62–74.

- 1 New generation of Earth observation satellites improves water quality monitoring.
- 2 MSI sensor aboard Sentinel-2A/B satellites provides high-resolution observations.
- 3 Sentinel-2 satellites were used to estimate water clarity in a reservoir surface.
- 4 Maps created with Sentinel-2 imagery provide rich information of water quality.

ACCEPTED MANUSCRIPT